

New implementation of explicit hydrometeor sedimentation in the Seifert-Beheng 2-moment bulk microphysical scheme

Ulrich Blahak, DWD

February 24, 2020

Contents

1	Theoretical considerations	1
1.1	Current explicit scheme	3
1.2	New improved explicit scheme	4
2	Idealized case studies	5
2.1	Simple 1D advection test with initial boxcar profile	5
2.2	Weisman-Klemp-type supercell simulation	12
3	Summary and conditional compilation for the new scheme	13
4	Note for ICON Users (24.02.2020)	13

1 Theoretical considerations

In the Seifert-Beheng 2-moment scheme, the sedimentation process is considered in a process splitting approach separately after all other microphysical processes (including saturation adjustment) at the very end of the physics time step. Numerically it is treated by a (very diffusive) first-order explicit scheme. The numerical diffusion of the scheme helps to alleviate some problems in a bulk description of sedimentation compared to the analytic solution of the original spectral equation.

Consider the pure bulk sedimentation problem

$$\frac{\partial \rho q}{\partial t} = -\frac{\partial}{\partial z} [v_{(\rho q)} \rho q] \quad . \quad (1)$$

Although we have written it in the form of a 1-moment scheme, it can be readily generalized to a two-moment scheme by adding an equation for a second moment and by letting v depend also on this second moment. For the sake of clarity, we will stick to the 1-moment description below, but the resulting formulae are applied to both moments of the scheme simultaneously.

After time integration from t_i to t_{i+1} and with $\rho q = \varphi$, one obtains the integro-differential equation

$$\varphi(t_{i+1}) = \varphi(t_i) - \frac{\partial}{\partial z} \left[\int_{t_i}^{t_{i+1}} v_{(\varphi(t))} \varphi(t) dt \right] = \varphi(t_i) - \frac{\partial}{\partial z} [\bar{P} \Delta t] \quad (2)$$

with $\bar{P} = \overline{v\phi}$ defining the time-averaged vertical sedimentation flux during a model time step $\Delta t = t_{i+1} - t_i$. v is always negative in our sedimentation problem.

Now let i be the time step index and k be the vertical grid level index of the COSMO-model (increasing from model top to bottom). If the fluxes \bar{P} are taken to reside on the vertical cell faces (model “half levels” in COSMO terminology), a direct simple mass-conserving discretization is

$$\varphi_k^{(i+1)} = \varphi_k^{(i)} - \frac{(\bar{P}_{k-1/2} - \bar{P}_{k+1/2}) \Delta t}{\Delta z_k} \quad (3)$$

with $\Delta z_k = z_{k-1/2} - z_{k+1/2}$, and the time integral for \bar{P} in Eq. (2) has to be evaluated numerically.

To prepare the numerical evaluation, we first transform this integral into a more useful formulation. Consider the flux \bar{P} through a height layer z_f . We exploit the fact that the explicit scheme uses “time-frozen” φ and v from time t_i and expand the integrand itself in an integral over a δ -function, which connects the time $t-t_i$ with the fall distance $v_{(\varphi(z,t_i))}(t-t_i)$ from which φ -contributions start to fall at t_i and height z to reach z_f at time t , i.e., $z = z_f + |v_{(\varphi(z,t_i))}|(t-t_i)$,

$$\begin{aligned} \bar{P}_{(z_f)} \Delta t &= \int_{t_i}^{t_{i+1}} v_{(\varphi(z_f,t))} \varphi(z,t) dt \approx \\ &\int_{t_i}^{t_{i+1}} v_{(\varphi(z_f+|v_{(\varphi(z,t_i))}|(t-t_i),t_i))} \varphi(z_f+|v_{(\varphi(z,t_i))}|(t-t_i),t_i) dt = \\ &\int_{t_i}^{t_{i+1}} \int_{z_f}^{\infty} v_{(\varphi(z,t_i))} \varphi(z,t_i) \delta_{[z-z_f-|v_{(\varphi(z,t_i))}|(t-t_i)]} dz dt \quad . \quad (4) \end{aligned}$$

Note that the well-known rarefaction wave at the tail of a “falling δ -peak” does not appear in our problem because we have chosen the fall velocity to be fixed during Δt . The lower limit z_f of the δ -integral is valid because flux contributions only stem from larger heights z in our sedimentation problem. The δ -function will help to avoid the problem, that the heights from which v and φ contribute to the integral depend on v itself.

If we use the following property of the δ -function,

$$\int_a^b \delta_{(x-x_0)} dx = \begin{cases} 1 & \text{for } x_0 \in [a, b] \\ 0 & \text{else} \quad , \end{cases} \quad (5)$$

change the order of integration in Eq. (4), apply the transformation $\zeta = z_f + |v_{(\varphi(z,t_i))}|(t-t_i)$, $d\zeta = |v| dt$ ($|v| = -v$; v does not explicitly depend on t in our scheme), $t = t_i \rightarrow \zeta = z_f$,

$t = t_{i+1} \rightarrow \zeta = z_f + |v|\Delta t$, and integrate over the δ -function in ζ , we obtain

$$\begin{aligned} \overline{P}_{(z_f)}\Delta t \approx & \\ & - \int_{z_f}^{\infty} \int_{z_f}^{z_f+v\Delta t} \varphi_{(z,t_i)} \delta_{(z-\zeta)} d\zeta dz = - \int_{z_f}^{\infty} \varphi_{(z,t_i)} \int_{z_f}^{z_f+v\Delta t} \delta_{(z-\zeta)} d\zeta dz = \\ & - \int_{z_f}^{\infty} \varphi_{(z,t_i)} F_{(z,v_{(z,t_i)})} dz \quad (6) \end{aligned}$$

with a masking function F defined as

$$F = \begin{cases} 1 & \text{for } 0 < z - z_f < |v_{(z,t_i)}|\Delta t \\ 0 & \text{else} \quad . \end{cases} \quad (7)$$

Note that there might be heights z above z_f from which φ -contributions reach z_f during Δt , and regions where this is not the case, depending on $v_{(z,t_i)}$. These regions can be alternating.

Eqs. (6) and (7) are our basis for evaluating the fluxes in Eq. (3) numerically.

The current scheme for this evaluation has problems when the local vertical Courant number is larger than 1, which usually happens close to the ground for relatively long model time steps and “fast sedimenting” species like rain drops, because the grid layers may get very thin close to the ground. Therefore, a new formulation has been developed and implemented into the COSMO-code of the 2-moment scheme.

The current and new method are described in the following. Here, z_f will be identified as $z_{k+1/2}$ and the explicit time index i will be dropped. Generally, the fluxes are computed according to a simple explicit first order upward scheme, i.e.,

$$v_{k+1/2}^{(i)} = v_k^{(i)} = \text{fct}(\varphi_k^{(i)}) \quad (8)$$

and $\varphi_k^{(i)}$ represents a constant value of φ within the vertical grid box Δz_k .

Note also, that a simple flux limiter is applied to avoid negative values after one sedimentation timestep, which destroys strict mass conservation of both the current and the new numeric scheme. Also, the mean fallspeeds for the 2 moments are bounded within a hydrometeor-type-dependent range. For example, number-density- and mass-density-fallspeeds for rain are clipped to a range of $[0.1, 20] \text{ m s}^{-1}$.

1.1 Current explicit scheme

This scheme is in effect if the code was compiled with no extra preprocessor flag or with the flag `-DSEDI_VECTORIZED` (vector-version for the NEC-SX9 vector-supercomputer).

In the current scheme, the fall velocity $v_{(z)}$ is approximated as $v_{k+1/2}$ for all heights above $z_{k+1/2}$. Therefore, the masking function F simplifies to a boxcar-function in the interval

$[z_{k+1/2}, z_{k+1/2} + v_{k+1/2}\Delta t]$ and Eq. (6) becomes

$$\bar{P}_{k+1/2}\Delta t \approx - \int_{z_{k+1/2}}^{z_{k+1/2}+v_{k+1/2}\Delta t} \varphi(z) dz \approx - \left[\sum_{l=0}^{N-1} \varphi_{k-l}\Delta z_{k-l} + \varphi_{k-N}(z_o - z_{k+1/2-N}) \right] . \quad (9)$$

N is the number of height levels whose cell faces are entirely within the maximum transport range of $z_o = z_{k+1/2} + |v_{k+1/2}|\Delta t$, and the last summand on the r.h.s. is the uppermost level contributing to the flux, whose upper face might be above the maximum transport range.

To determine N , the code implementation makes use of a recurrence relation a local Courant number,

$$c_{k-l} = (c_{k-l+1} - 1) \frac{\Delta z_{k-l+1}}{\Delta z_{k-l}} \quad \text{with} \quad c_k = \frac{|v_{k+1/2}|\Delta t}{\Delta z_k} = \frac{z_o - z_{k+1/2}}{\Delta z_k} . \quad (10)$$

It is $c_{k-l} > 1$ for $i < N$ and $c_{k-N} = \frac{z_o - z_{k+1/2-N}}{\Delta z_{k-N}}$, therefore we can rewrite Eq. (9)

$$\bar{P}_{k+1/2}\Delta t \approx - \sum_{l=0}^N \varphi_{k-l} \min[c_{k-l}, 1] \Delta z_{k-l} \quad (11)$$

and stop the summation at the index i where c_{k-i} becomes < 1 for the first time.

1.2 New improved explicit scheme

This scheme is in effect if the code was compiled with the flag `-DSEDI_NONVECTORIZED_BOXTRACKING`. There is no vectorized version yet.

The new explicit scheme directly discretizes Eqs. (6) and (7), without any approximation of $v(z)$ by $v_{k+1/2}$:

$$\begin{aligned} \bar{P}_{k+1/2}\Delta t &\approx - \sum_{l=0}^{k-1} \varphi_{k-l} (z_{up} - z_{low}) \\ z_{up} &= \min [z_{k+1/2-l-1}, z_{k+1/2} + |v_{k-l}|\Delta t] \\ z_{low} &= \min [z_{k+1/2-l}, z_{up}] . \end{aligned} \quad (12)$$

Note that in this form, the summation of each flux in level $k + 1/2$ runs from level k to the top of the model domain, but there are only non-zero contributions from those boxes $k - l$ whose lower cell face fullfills $z_{k+1/2-l} < z_{k+1/2} + |v_{k-l}|\Delta t$. This makes it more costly than the current scheme from Sec. 1.1. However, if the summation of each flux for each non-zero contribution is organized differently, the same efficiency as for the current scheme is achieved. For this, the algorithm checks for each box k to which fluxes through below layers $z_{k-1/2+l}$ it contributes. This search is continous and enables a proper stopping criterion for the inner

loop over l . Basically, layer k contributes if its lower cell face falls below layer $z_{k-1/2+l}$ during Δt .

In algorithmic notation:

```

 $\bar{P}_{1/2:k_{end}+1/2} = 0$  ;
do  $k = 1, k_{end}$ 
   $l = 0$  ;
  while  $z_{k+1/2} - |v_k|\Delta t < z_{k+1/2+l}$  and  $k + l \leq k_{end}$  do
     $z_{low} = z_{k+1/2} - |v_k|\Delta t$  ;
     $z_{up} = \min [z_{k+1/2-1} - |v_k|\Delta t, z_{k+1/2+l}]$  ;
     $\bar{P}_{k+1/2+l} \Delta t = \bar{P}_{k+1/2+l} \Delta t - \varphi_k (z_{up} - z_{low})$  ;
     $l = l + 1$  ;
  end while
end for

```

A more suitable formulation for the code can be derived by introducing the pure translative transformation $z' = z + |v_k|\Delta t - z_{k+1/2}$ and the fact that $z_{k+1/2+l} = z_{k+1/2} - \sum_{m=1}^l \Delta z_{k+m}$, so that the final algorithm is

```

 $\bar{P}_{1/2:k_{end}+1/2} = 0$  ;
do  $k = 1, k_{end}$ 
   $l = 0$  ;
   $\Delta_{sum} = 0$  ;
  while  $\Delta_{sum} < |v_k|\Delta t$  and  $k + l \leq k_{end}$  do
     $z_{low} = 0$  ;
     $z_{up} = \min [\Delta z_k, -\Delta_{sum} + |v_k|\Delta t]$  ;
     $\bar{P}_{k+1/2+l} \Delta t = \bar{P}_{k+1/2+l} \Delta t - \varphi_k (z_{up} - z_{low})$  ;
     $l = l + 1$  ;
     $\Delta_{sum} = \Delta_{sum} + \Delta z_{k+l}$  ;
  end while
end for

```

where Δ_{sum} represents the term $\sum_{m=1}^l \Delta z_{k+m}$.

2 Idealized case studies

2.1 Simple 1D advection test with initial boxcar profile

To compare the current and the new sedimentation algorithm, a simple 1D test problem has been set up within the idealized framework of COSMO. 64 vertical levels up to 5000 m have been chosen with the distribution of vertical level thicknesses as function of level index shown in blue in Fig. 1 (red: COSMO-DE standard levels). At initial time, rain water mixing ratio q_r has been set to 0.001 in a boxcar-like fashion from level 20 to 40. The mass specific number concentration n_r has been chosen in a way that a mean mass diameter of 1 mm results. Note that the profile is not exactly boxcar-like in terms of rain density $rhoq_r$ because of the density decrease with height, but this level of detail is unimportant for the test case. Such a test

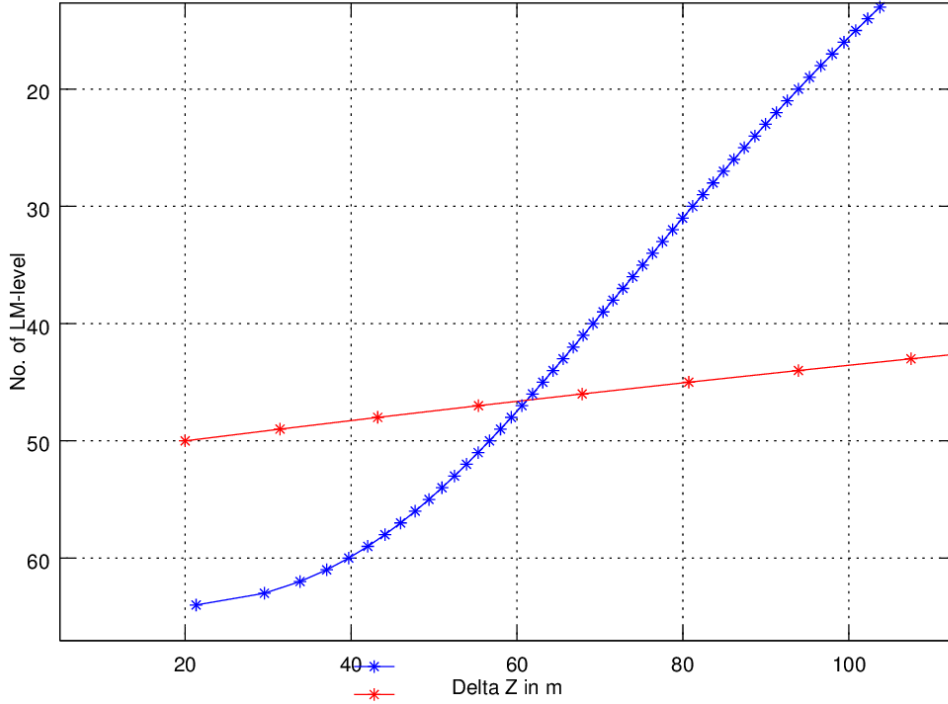


Figure 1: Blue: vertical layer thicknesses in m (X -axis) as function of COSMO model vertical layer index (Y -axis) for the idealized experiments in Sec. 2.1.

case is considered to be very extreme for any numerical scheme because of the sharp gradients across the two shocks.

The initial profiles of $T_{(z)}$, $q_{v(z)}$ and $p_{(z)}$ were chosen similar to Weisman and Klemp (1982), except that the relative humidity is constant at a value of 95% everywhere. This high value was chosen in order to minimize raindrop evaporation. An alternative would have been to switch off this process in the microphysics code, but this has not been done here.

Simulations are performed with time steps of 1, 10 and 30 s to investigate the influence of the vertical Courant number on the results, especially close to the ground, where the model layers usually become rather thin. The resulting mean fallspeeds from q_r and n_r are within a range of 5 - 10 m s⁻¹. This means that, considering the layer thicknesses from Fig. 1, at 1 s timestep the Courant numbers are well below 1, at 10 s they are in a range of about 1 - 3 and at 30 s they can reach about 10 close to the ground. This covers weak, moderate and high Courant number regimes.

Fig. 2 shows the development of the vertical q_r profile with time for the most extreme case with $\Delta t = 30$ s. The current scheme in the upper panel develops very high and very unrealistic peaks at the forefront of the falling rain, which are due to the fact that the flux at the lower cell

face of the layer right below the “first drops” is 0 because the fallspeed in the flux calculation is very low (lower threshold of 0.1 m s^{-1}) due to $q_r = 0$. A similar behaviour is expected also for n_r , but with a lower fallspeed. Therefore, the rain signal can propagate downwards no more than one height level per timestep, and there is an artificial, grid-structure-induced “rain congestion”. Due to the nonlinear dependence of the fluxes on q_r and n_r , such peaks are self-amplifying with time and fall distance, which is clearly visible in the upper panel.

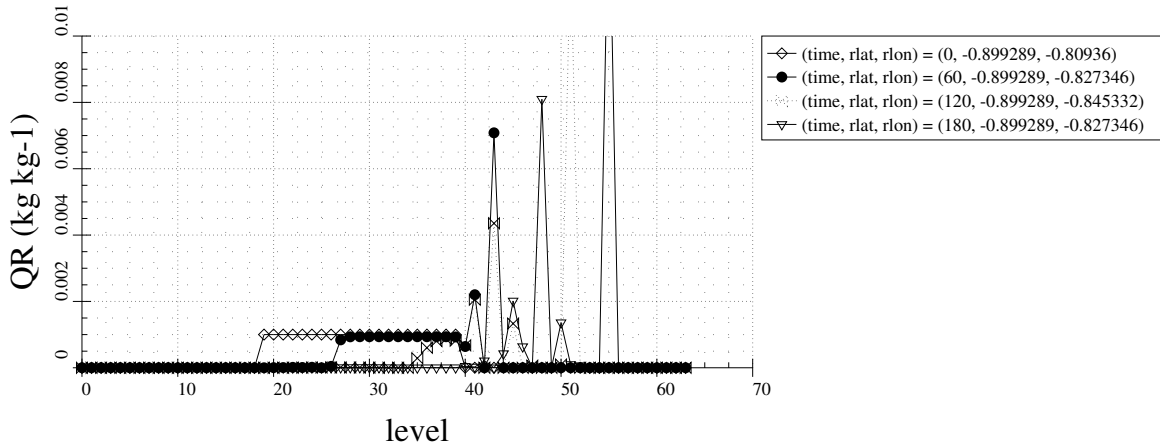
The new scheme (lower panel) does not show such drastic peaks, because the correct fallspeed for each layer enters the flux calculation. The signal of the “first drops” can pass more than one height layer per timestep. However, some noise is still visible, presumably because the sedimentation of the 2 moments is coupled through the dependence of both moment fallspeeds on both moments, and errors (peaks) might be self-amplifying. The situation is however much improved compared to the current scheme.

Fig. 3 compares timeseries (sec) of surface rain rate (mm h^{-1}) for different timesteps (panels) and the two schemes (red: current scheme, green: new scheme). The upper panel is for $\Delta t = 1 \text{ s}$, the middle panel for 10s and the lower panel for 30s. At 1s (Courant number always < 1), both schemes show exactly the same curve with a smooth peak at around 400s of 9 mm h^{-1} . At 10s the current scheme develops very strong and interrupted rainrate pulses, which are a consequence of the self-amplifying peaks in the q_r profile. The current scheme also develops some pulses and also deviates from the reference solution with $\Delta t = 1 \text{ s}$, but by far not so strong as the current scheme. Qualitatively it is the same also for $\Delta t = 30 \text{ s}$ in the lower panel. But here the current scheme not only develops strong isolated pulses but also the first drops reach the ground more than 200s later, a consequence of the no-more-than-one-height-level-per-timestep rain front propagation.

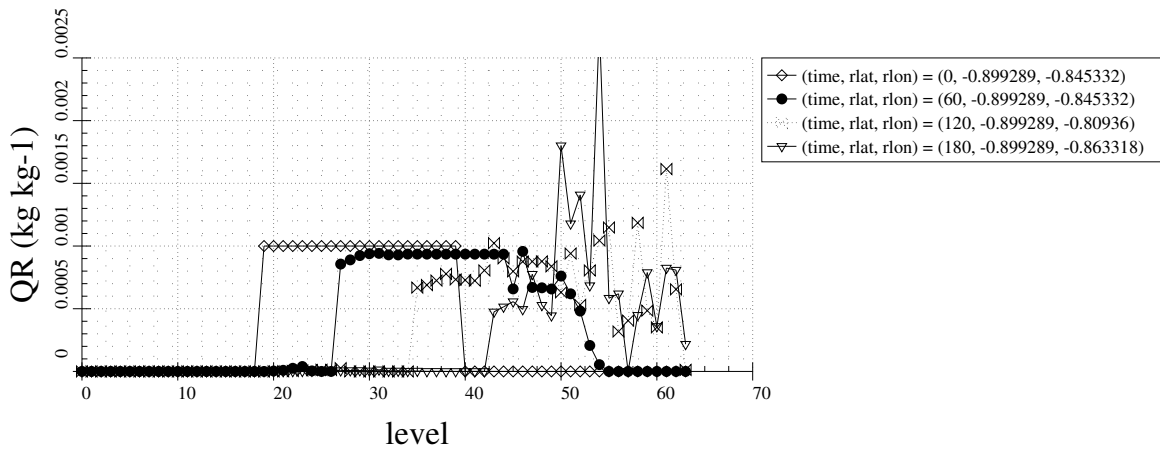
The same curves are again shown in Fig. 4 but re-grouped according to the numerical scheme. The left panel is for the current scheme and the right panel for the new scheme. Whereas the current scheme clearly has severe problems with rain timing and isolated pulses as soon as local Courant numbers are considerably larger than 1, the new scheme does a better job, although some problems with signal deformation and (weaker) pulses are visible. A distinct feature of the new scheme is the first “flank” of the rain peak. Although the first rain signal at the ground appears about at the same time, the rainrate increase up to the first peak is sharper for longer timesteps. This is perhaps a consequence of the timestep dependence of numerical diffusion, which increases with the number of scheme calls and is therefore more active for shorter timesteps.

For reference and to compare our explicit sedimentation schemes qualitatively with the numerically more stable semi-implicit scheme of the COSMO 1-moment schemes, the simulations were repeated but with using the COSMO “graupel” scheme. Note that we have to expect a different behaviour of the profiles and the rainrate time series because we are dealing with a 1-moment sedimentation problem and not with a coupled 2-moment system. Peaks and pulses might not be as self-amplifying as in a two-moment scheme. However, Fig. 5 (comparable to Fig. 2) demonstrates that the semi-implicit scheme is much more stable with respect to large Courant Numbers and does not produce unrealistic peaks and pulses. Also, the time series of the rainrate at the ground is nearly independent of the timestep, even for very large local Courant numbers (Fig. 6).

Therefore, although the new explicit scheme seems to behave reasonable and much better compared to the current scheme, the re-implementation of the two-moment framework into a semi-implicit solver similar to the COSMO 1-moment schemes seems desirable.



specific rain content



specific rain content

Figure 2: Vertical profile of q_r as function of model layer index k at initial time, 2 min, 4 min, and 6 min, for the simulation with the “very long” timestep of 30 s. With time, the profile shifts from left to right, more and more departing from the initial boxcar-profile. **Upper panel:** current sedimentation scheme. **Lower panel:** new scheme.

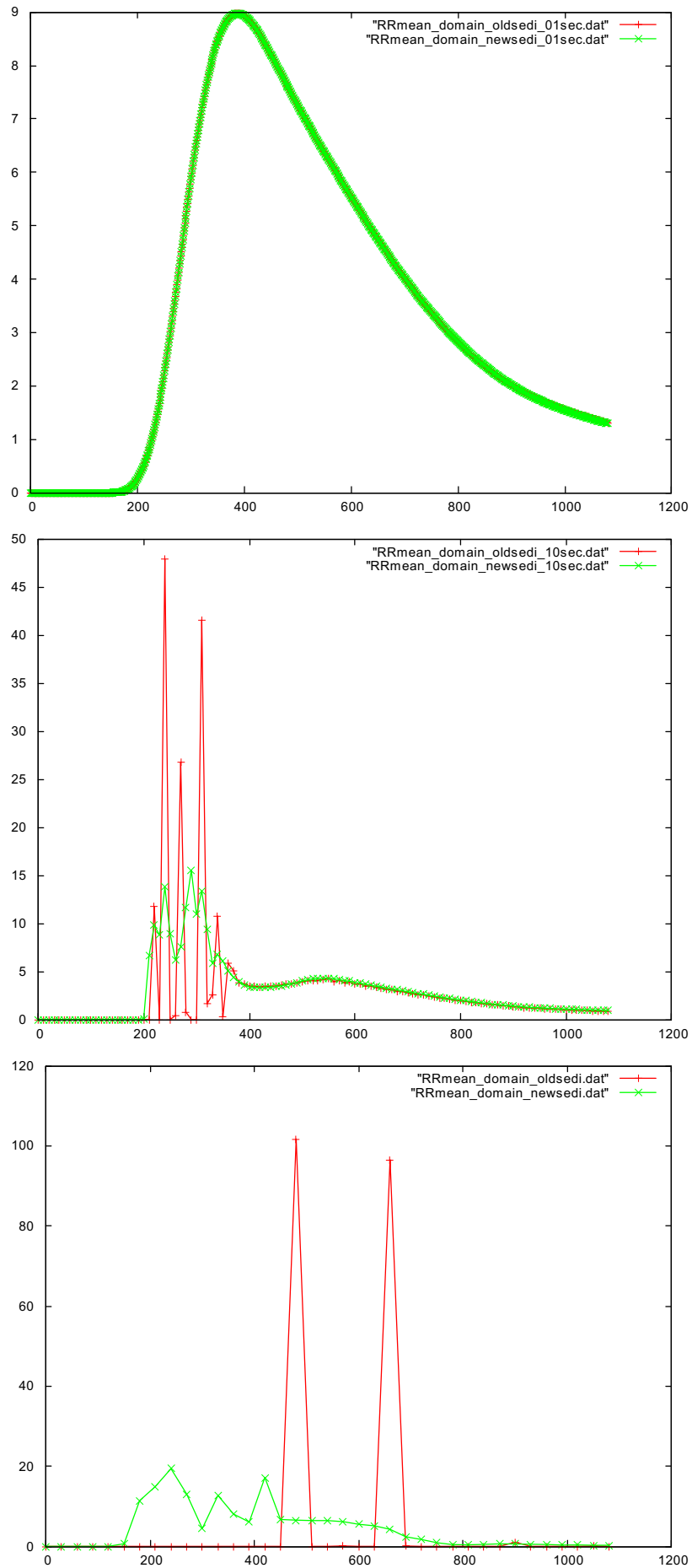


Figure 3: Timeseries (sec) of surface rain rate (mm h⁻¹) for different timesteps (panels) and the two schemes. Red: current scheme, green: new scheme. The upper panel is for $\Delta t = 1$ s, the middle panel for 10 s and the lower panel for 30 s

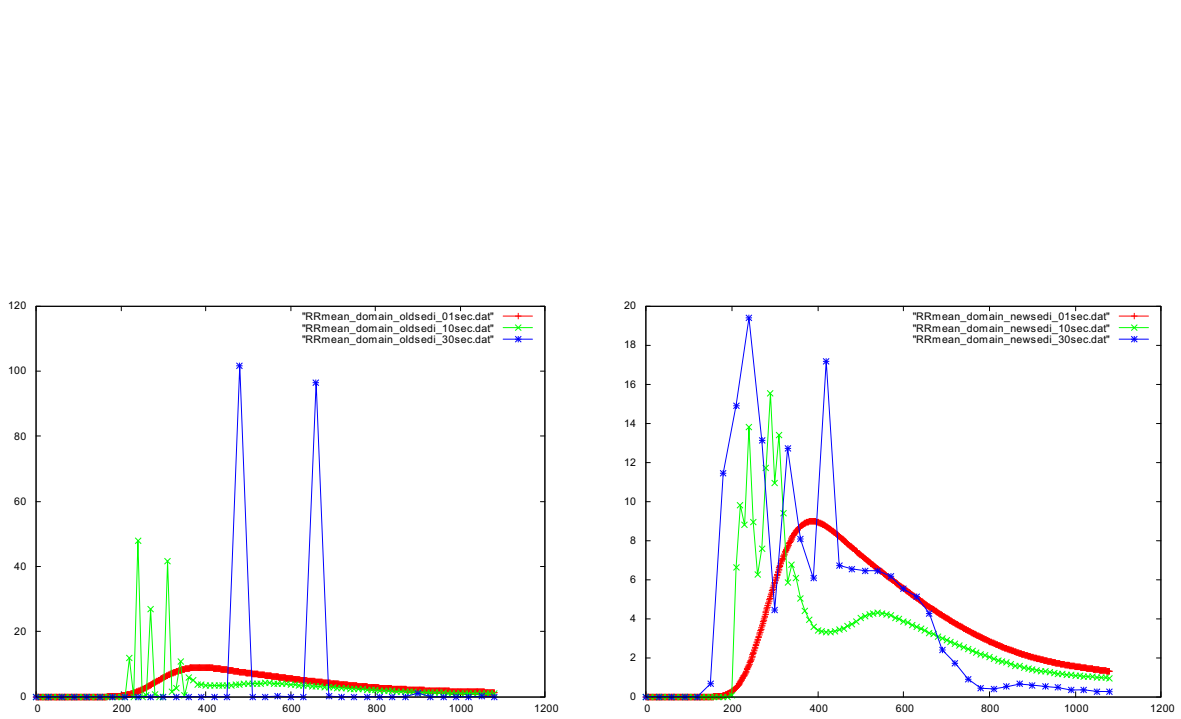
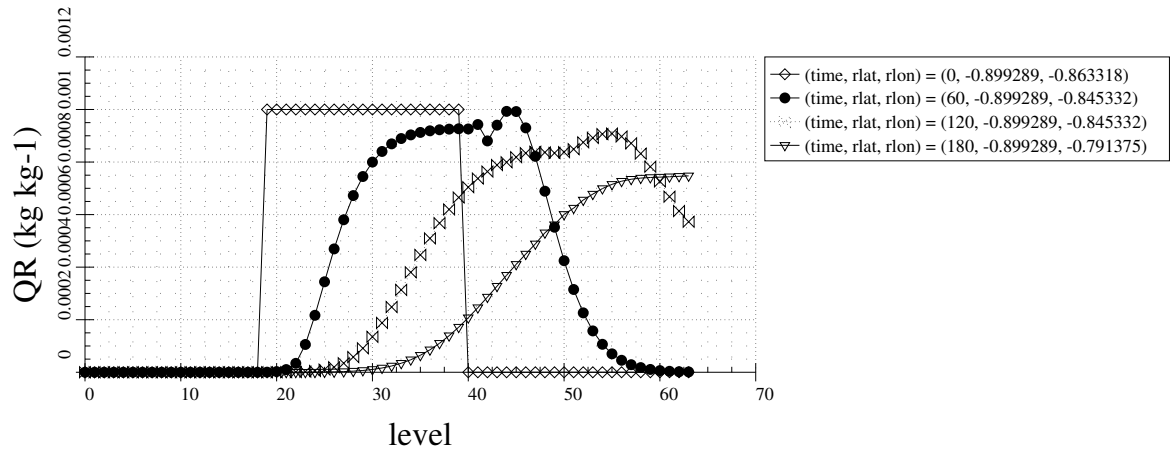


Figure 4: Same time series as in Fig. 3 but re-grouped according to the numerical scheme. Left: old scheme, right: new scheme.



specific rain content

Figure 5: Similar to the panels in Fig. 2, but for the COSMO standard microphysics semi-implicit time integration scheme, as described in the COSMO-Dokumentation Part II.

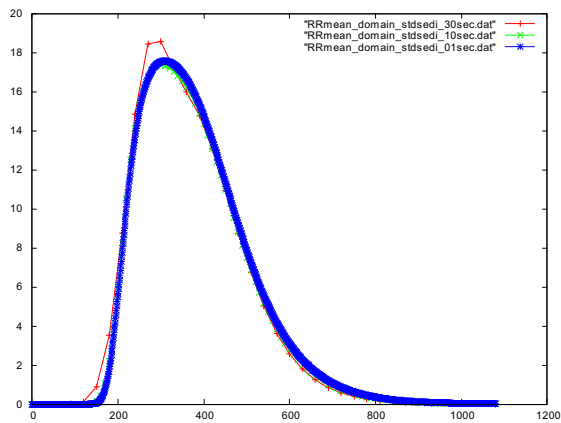


Figure 6: Similar to the panels in Fig. 4, but for the COSMO standard microphysics semi-implicit time integration scheme, as described in the COSMO-Dokumentation Part II.

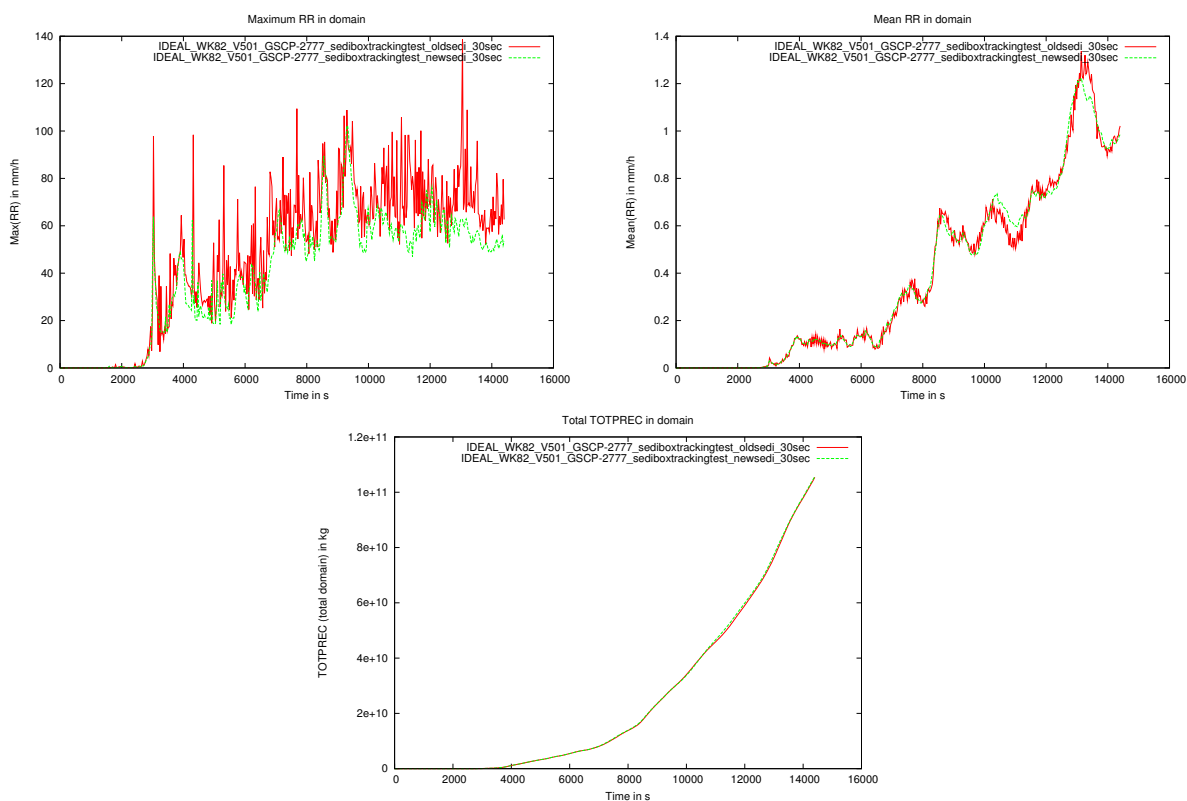


Figure 7: Figures for the Weisman-Klemp supercell simulation. See text for description.

2.2 Weisman-Klemp-type supercell simulation

A more realistic type of 3D deep convective cloud simulations are idealized Weisman-Klemp-type simulations. In fully periodic domain, potentially unstable initial conditions are specified and a large “warm bubble” in the boundary layer (present in the initial condition) leads to a strong convective updraft and a subsequent development of a deep convective system. Depending on *CAPE* and wind shear, single-, multi- or supercell type storms develop.

To compare the current and new sedimentation scheme, simulations with a maximum specific humidity of 14 g/kg and with a windspeed of 20 m s^{-1} in the upper troposphere have been performed. Horizontal grid length and vertical layer specification is exactly equal to the COSMO-DE setup (2.8 km, 50 layers), and the domain size is 200 by 200 grid points. The timestep has been set to 30 s, which is slightly larger than in COSMO-DE, but the windspeeds are comparatively low so that this timestep does not pose serious stability problems for the dynamics. Vertical sedimentation Courant numbers are however $\gg 1$, especially close to the ground.

In contrast to the more simple test in the last section, here all hydrometeor types are involved and the vertical hydrometeor profiles are more realistic, presumably with smaller vertical gradients.

To summarize the results, Fig. 7 compares time series of domain maximum precipitation rate (upper left panel), domain mean precipitation rate (upper right panel), and total domain and time accumulated precipitation (lower panel) for the current and new scheme. The current

scheme (red lines) clearly shows signatures of a noisy and “nervous” maximum precipitation rate, which can be attributed to the erroneously pulsed behaviour of the sedimentation scheme associated with too high local Courant numbers. In the new scheme, these pulses do not occur and the time series of maximum precipitation is much smoother.

Domain mean- and total accumulated precipitation are however not affected. Because both schemes are (almost) mass conserving, the pulses caused by the current scheme average out in time and/or space. However, the fine structure of the spatial precipitation distribution is different among the simulations (not shown).

3 Summary and conditional compilation for the new scheme

There has been an update of the explicit sedimentation scheme in the Seifert-Beheng two-moment microphysical scheme. The new method mitigates some problems with the old scheme, if the timestep is larger than about 10 s and the vertical courant number close to the ground becomes much larger than one. Users should now switch to the new scheme by changing a preprocessor flag in their compiler options:

- Delete `-DSEDI_VECTORIZED`
- Add `-DSEDI_NONVECTORIZED_BOXTRACKING`

The only exception is if users are running on a NEC-SX vector-supercomputer. Here, the new scheme does not properly vectorize and one gets a serious penalty in runtime. Maybe the new scheme will be vectorized in a future code version, but up to now one should continue to use `-DSEDI_VECTORIZED` in this case.

However, although the new explicit scheme seems to behave reasonable and much better compared to the current scheme, the re-implementation of the two-moment framework into a semi-implicit solver similar to the COSMO 1-moment schemes seems desirable. But this would require a major code re-write. Also, some performance problems could occur because in this solver, the terminal fall speeds of the hydrometeors have to be computed twice per timestep, which can be somewhat expensive.

4 Note for ICON Users (24.02.2020)

The new explicit sedimentation scheme has been ported to the ICON-version of the two-moment scheme in February 2020. The choice of the sedimentation scheme is internally hardcoded in ICON to the new scheme by internal switches `lboxtracking=.TRUE.` in `mo_2mom_mcrph_processes.f90`. Though the old scheme is not recommended any more, the user might switch it on manually by setting all occurrences of `lboxtracking=.FALSE.` in that module.

In ICON there is also a vectorized version of the new scheme, in order to run efficiently on the upcoming NEC Aurora system of DWD. The vectorized version is chosen automatically on the NEC Aurora by one of the (hopefully automatically defined) preprocessor flags

- `-D__NECSX__`
- `-D__SX__` or
- `-D__NEC_VH__` .

In contrast to COSMO, in ICON the two-moment scheme has been integrated into the semi-implicit solver framework (thanks to Axel Seifert!). The semi-implicit solver can be activated by setting the internal switch `explicit_solver=.FALSE.` in `mo_2mom_mcrph_driver.f90` and recompile. By default, this switch is set to `.TRUE.` and the explicit solver with explicit sedimentation is used.